Chaos in the Solar Cycle: using data to drive predictions

Matthew Young

May 21, 2012

Abstract

This report presents first steps at applying chaos theory to the solar activity cycle. We provide brief reviews of the history of sunspot records, the mathematical framework of chaos theory, and solar dynamo theory. Finally, we present results of nonlinear analysis of solar motion and propose that further research focus on characterizing local Lyapunov exponents of solar dynamics.

1 Introduction

The Sun is a mass of incandescent gas [45] whose chief role, as far as life on Earth is concerned, is to fuse hydrogen into helium and produce life–sustaining energy in the process. If that were its only pass–time, however, the Sun would be a luminous, glorified one–trick pony. The Sun also produces neutrinos in its core, exhibits many modes of oscillation throughout its volume, and fires off various ejecta from its surface in the form of electromagnetic energy and plasma. We still do not completely understand all the dynamical processes that occur inside the Sun, but we know that its inner goings–on are intimately connected to our lives in ways biological, spiritual, and technological. We also know that its inner workings are not as simple as [45] implies: it is a fluid sphere whose outer thirty percent rotates differentially while its core rotates more or less uniformly, it exhibits large–scale meridional flows and small–scale turbulence, and it goes through two noteworthy cycles: The 11–year (Schwabe) activity cycle, and the 22–year (Hale) magnetic cycle.

Previous studies (e.g. [23] and [36]) have attempted to explain the variation in solar cycles by appealing to an argument based on planetary tidal forces. The basic line of such an argument is that the gravitational pull on some region of Sun due to all (or some subset) of the planets results in the cyclical nature of solar variability, much as the Moon causes ocean tides on Earth. Apparent similarities between the orbital periods of Jupiter and Saturn, and the 11–year Schwabe cycle make the notion of planetary tides enticing, but certain authors (e.g. [39] and [7]) have provided strong cases against linear planetary forcing arguments.

In this paper, we propose to apply the joint frameworks of chaos theory and nonlinear time series analysis to solar data in order to further our understanding of the dynamics of

the Sun. Naturally, we must begin by answering the question, "is solar motion chaotic?" but once we have established that it is, we may move on to the more intriguing challenges of exploring nonlinear connections between chaos in solar motion and other objects in the solar system, and using knowledge of solar dynamics to work toward a method of predicting future solar activity.

2 History and Recent Work

Before embarking on a quantitative analysis of chaos in solar activity and dynamics, let us trace the observational history of solar activity through the development of the sunspot record. We will follow this brief history with some examples from the recent literature of how analysis of solar activity is used to benefit the scientific community and society as a whole.

2.1 Early Work

Theophrastus of Athens, a student of (and eventual successor to) Aristotle, made the first recorded observation of a sunspot when he identified them as indicators of rain in a meteorological treatise circa 325 BC. In fact, he referred to them casually enough in his writing that we may presume that sunspots were by then already familiar sights [46]. At the time of Theophrastus and up until the invention of the telescope in the 17^{th} century, those interested in the Sun could only observe sunspots during periods of persistent haze or smoke on the horizon. This would have been enough to obscure enough visible light to allow small dark spots on the surface of the Sun to stand out, though it could not have provided any protection from ultraviolet radiation to shield the observer's eyes from long–term harm. In this sense, as would later be true in the case of early studies of radioactive materials, naïvité was a boon to science.

The advent of the telescope in Europe meant that scholars and amateur astronomers could more easily track the occurrence rates and motion of sunspots, without having to wait for a sand storm to blow through, or for an entire city to catch fire. It is not surprising that Galileo Galilei had a hand in the sunspot game, but he was not the only interested observer. While he had many contemporary budding heliophiles, Galileo fought most bitterly with Christoph Scheiner over who deserved precedence with regard to the first observation of a sunspot through a telescope, among other matters [40]. It is interesting to note that Scheiner first used the transit of sunspots across the solar disk to determine that the Sun's rotational axis is tilted 7.5° from the normal to the ecliptic plane, but when Galileo used the deformation in this tilted transit to argue in favor of a heliocentric solar system, Scheiner (a Jesuit priest) disagreed. Scheiner, for his part, invoked an additional precession of the Sun's axis to maintain the geocentric viewpoint [46]. History has borne out Galileo's hypothesis, but unfortunately, the contemporary religious climate did not hold such an opinion in high regard.

William Herschel is credited with developing the first precise past record in 1801 of both the presence and absence of sunspots, and with forwarding the conjecture that an absence of sunspots coincided with higher–than–usual wheat prices in England. For his efforts, the Royal Society of England lavished him with ridicule, though his fate was certainly more pleasant than that of Galileo [40]. Given the awe with which the Sun has been regarded for millennia, this certainly could not have been the first time that perceived solar activity was blamed for events on Earth. However, it was the first step toward methodically correlating sunspot activity with climate–related events on Earth (presuming, of course, that the high wheat prices were due to a poor growing season, which was itself due to weather–related phenomena).

Next came Heinrich Schwabe. As is wont to happen during the course of carefully scientific inquiry, Schwabe discovered the sunspot cycle around 1840 when he was searching for something completely different. At the time, he estimated it to be ~ 10 years. Schwabe had the suspicion that there was an object orbiting the Sun inside the orbit of Mercury, and was therefore making careful observations of any dark spots on the solar disk that would indicate the presence of another body [46]. Fortunately for us, sunspots and small planets look very similar, and he was able to make a substantial discovery, despite the fact that it was not the discovery he hoped for.

By the late 1850s, Richard Carrington was stationed at the Red Hill Observatory in Surrey, England, where he recorded occasions in which a dark sunspot would flash white, and a magnetic signature (e.g. the deflection of a compass needle or the interruption of telegraph service) would be registered on Earth [40]. In a way, these observations are the logical successors to Herschel's conjecture that sunspot patterns are somehow linked to events on Earth that affect daily life. Carrington and Gustav Spörer independently made two of the most important contributions to heliophysics since Schwabe's discovery of the solar cycle: The first is that sunspots move equatorward throughout the solar cycle; the second is that spots near the equator rotate more quickly than spots at higher latitudes, implying that the Sun rotates differentially, and providing evidence that the Sun is a fluid [46]. Spörer is best known for the former (called the "Spörer Sunspot Law") and Carrington is best known for the latter (called "Carrington rotation"). This period also saw Rudolf Wolf, who is best known for establishing a "relative sunspot number" (which he used as a way to normalize world–wide sunspot counts), then employing those normalized counts to trace solar cycles back as far as he could. By that time, the heliophysics community had since refined their estimates to place the solar cycle closer to 11 years, so he settled on the cycle from 1755–1766 as Cycle 1. We still employ Wolf's numbering scheme today.

These observations, especially the polar–to–equatorial sunspot drift, set the stage for Edward Maunder at the turn of the twentieth century. Maunder was well aware of Spörer's work and he made a point in his 1904 paper "Note on the Distribution of Sun–spots in Heliographic Latitude 1874–1902" to defend Spörer's assertion that the mean sunspot location migrates equatorward against certain members of the scientific community who, Maunder felt, misunderstood Spörer's point [27]. Maunder's conclusions also lent credence to obser-

vations made by Wolf around the same time. Figure 1 reproduces Figure 8 of Maunder's 1904 paper. It is the first occurrence of the "Butterfly diagram" method of representing the distribution of sunspots with latitude over the course of one or more solar cycles, an image now very familiar to members of heliophysics community. This representation scheme was one of Maunder's chief contributions to the study of solar activity, but perhaps the most ubiquitous reference to him within the subject of the Sun–Earth connection lies in the name given to the period 1645–1715: "The Maunder Minimum". Maunder had identified a dearth of sunspots in telescopic records during this time, but received most of his praise posthumously, when Jack Eddy compiled a thorough review of the data available to him in 1976 and formally named that period of anomalously low solar activity after Maunder [13]

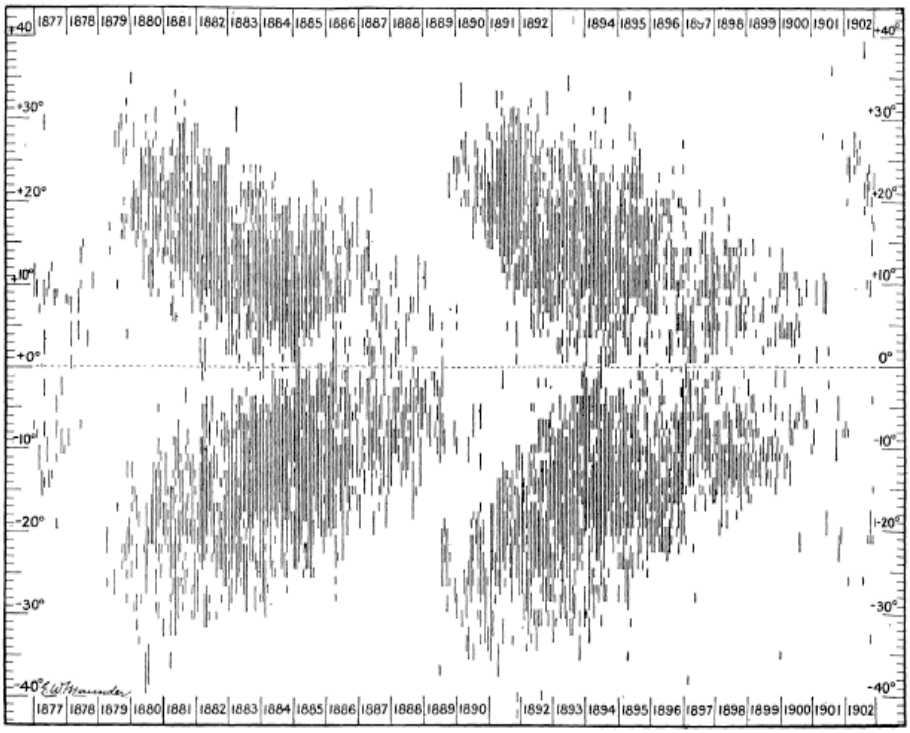

FIG. 8.—DISTRIBUTION OF SPOT-CENTRES IN LATITUDE, ROTATION BY ROTATION, 1877–1902.

Figure 1: The original image from Maunder's 1904 paper, "Note on the Distribution of Sun–spots in Heliographic Latitude 1874–1902" [27]. The winged shape gives this "Butterfly diagram" its name. In the diagram, time (in years) moves from left to right while latitude on the solar surface (-40° to +40°) moves from bottom to top.

Maunder was also interested in investigating the relationship between sunspots and geomagnetic activity once studied by Wolf and Edward Sabine in the mid–nineteenth century [40]. Whether or not he satisfied his curiosity, it was his contemporary George Hale who took the crucial next step toward connecting sunspots to magnetism. In 1908, Hale discovered Zeeman splitting in spectral lines that he identified with sunspots. In doing so, he determined that the mean magnetic field of a sunspot is $\sim$ 2900 G (0.29 T) and he proposed that this magnetic field originates in the vortex motion of a sunspot. Since his photographic evidence suggested that all sunspots are vortices, it must follow that all sunspots give rise to a magnetic field [17]. The magnetic field intrinsic to a sunspot is not itself the cause of the solar events such as coronal mass ejections (CMEs) and solar flares that disrupt life on Earth, but they are locations on the surface of the Sun out of which the Sun's magnetic field peaks. Thus they were early evidence of the Sun's powerful, persistent magnetic field [46].

With that note, we must make the transition from thinking of sunspots as focal events to thinking of sunspots as proxies for other events more meaningful to life on Earth. The discovery of the sunspot cycle is a testament to good scientific practice, and its analysis over a century and a half has met with wonder and has begotten further interest in heliophysics, but sunspots alone do not drive space weather. Their cycle is, nevertheless, an important indicator of the ebb and flow of solar activity. Most notably, we have come to learn that sunspots are also regions of high–energy activity, and are the seats of solar flares. Solar flares are sources of x–ray radiation that influences Earth's ionosphere and are typically followed by coronal mass ejections (CMEs) that can cause geomagnetic storms if they are directed Earthward [44]

2.2 Recent Applications

Late October into early November 2003 was a period of impressive solar activity referred to within the space science community as the Halloween storms (*cf* [37], [15]). This activity had noticeable electromagnetic effects, including momentarily stripping plasma away from the region of space surrounding the Earth, and disrupting the Earth's magnetic field and producing auroral displays. In addition to those effects on the plasma environment, which are to be expected to some degree, the Halloween storms produced two solar flares that were associated with measurable changes in the density of neutral molecules in the atmosphere [43].

Manned space missions pose a threat of high doses of radiation to the astronauts involved, due to the fact that they are no longer shielded from high–energy particles by the Earth's magnetosphere. Mars is a natural destination for manned flights, but the duration of the required trip would cause the flight personnel to be exposed to amounts of hazardous radiation nearly equal to the career limit levels established by NASA [42]. Such exposure to background radiation is reasonably well–understood; however NASA still lacks the ability to predict solar flares that could expose astronauts to an additional high dose of radiation

(*ibid*).

Beyond the scope of the electromagnetic effects of high–energy bursts of plasma and x–ray radiation, authors have proposed various links between changes in solar activity and changes in human health. Preka–Papadema *et al.* examined procedural records from emergency rooms in two Greek hospitals during scattered months from 2000 through 2006 (Cycle 23). They concluded that cases of cardiological trauma, neurological trauma, and burns, as well as cases related to oncology and pathology increased during periods of heightened solar activity [34]. Other authors reported that there is a statistically significant link between certain terrestrial weather cycles, and planetary and solar wind geomagnetic indicators [16]. Those authors go on to claim that they have found similar cycles "in over 2500 years of international battles, in 2189 years of tree rings, in around 900 years of the aurora, and in human psychophysiology" (*ibid*). A third set of authors identify statistically significant periods in cervical epithelial abnormalities matching the approximately 11–year sunspot cycle [21]. They proposal various possible mechanisms, including the effect of changing geomagnetic fields on iron in the human body, flare–related radiation incident upon the surface of the Earth, and subconscious reactions to changes in terrestrial weather induced by space weather events. However, they acknowledge that a correlation between solar cycles and human health cycles does not necessarily mean that a causal effect exists.

As proposed effects of solar activity move further and further from space weather, it is natural to the scientific community (especially the space science community) to greet them with skepticism. However, only a narrow mind will turn away such propositions categorically, and we must not make that mistake. The trouble is that even effects on terrestrial weather are "indirect" and thus "very complex" [44], so that a causal link is difficult or impossible to make. That difficulty does not mean we should not continue to study the relationship between solar activity and life on Earth.

3 Characteristics of Chaotic Systems

Thus far, we have considered observations of sunspots and what their relative presence or absence indicates about the current level of solar activity. We have furthermore examined the effect of solar activity on the near–Earth environment, and possible impacts on terrestrial life. However, we have not yet characterized the increase and decrease in solar activity in a precise way. The purpose of this paper is to connect evidence of the variability of solar activity cycles (in the form of sunspot counts) to predictable physical parameters in a quantitative way in order to further our ability to predict the nature of future solar activity.

Simply put, the Sun appears to exhibit characteristics of a chaotic system. Our first task, then, is to precisely define what we mean by the terms "chaos" and "chaotic system". Deterministic chaos is the motion of a system whose time evolution has a sensitive dependence on initial conditions. We may contrast this with randomness, which describes the

motion of a system in which the present state has no causal connection to the previous one [47]. As a simple example of this contrast, consider the following two dynamic systems: a coin toss, and the waterwheel shown schematically in Figure 2. Both systems are subject to the laws of classical physics and both evolve in time according to mathematical formulæ that can be written down. However, the coin toss is random and the waterwheel is chaotic. In the former case, each flip of the coin carries no information about the previous flip, and begets no knowledge of the result of the subsequent flip. There are dynamic quantities at work during each toss (e.g. the angle of the coin relative to the flipper's thumb pre–toss, the weight of coin, etc.), but once the coin lands and the outcome is recorded as "heads" or "tails", the system resets. The net result of many tosses is subject to the laws of probability alone.

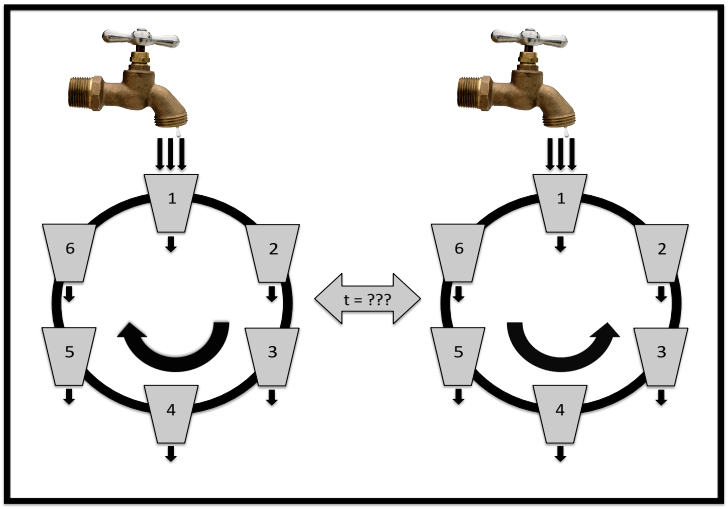

Figure 2: Schematic representation of a chaotic waterwheel. The water flows in from the faucet, filling cup the cup beneath, and drains from the bottom of each cup at a specified constant rate. The wheel will begin turning left or right when the weight of water in cup #1 overcomes the friction forces holding the wheel still. The distribution of water mass will determine the rate and direction of rotation, which will be chaotic for certain rates of flow and drainage.

In contrast, the position and velocity of a cup on the waterwheel at time t_i (which, as a pair, are analogous to "heads" and "tails" after a given coin flip) depend on the position and velocity at time t_{i-1}. This should be intuitive, since the matter that makes up the waterwheel can not simply disappear from one location and appear at another, nor can otherwise absent energy suddenly cause a jump in the momentum of that matter.

Edward Lorenz found, in the early 1960s, that it is possible to force certain hydrodynamical systems mechanically or thermally (he studied a system that involved both) such that the system exhibits either periodic, quasi–periodic, or non–periodic behavior "when there is no obviously related periodicity or irregularity in the forcing process" [26]. He applied simplifying assumptions to a system in which a cylindrical basin of water was rotated mechanically and subjected to a radial thermal gradient, and derived the following system of equations:

$$\dot{x} = -\sigma(x - y) \quad (1)$$
$$\dot{y} = -xz + rx - y \quad (2)$$
$$\dot{z} = xy - bz \quad (3)$$

where a dot indicates a time derivative and σ, r, b are parameters. Despite the presence of water and mechanical forcing in the Figure 2 system, this is not the system that Lorenz studied. What is remarkable, however, is that Equations 1–3 exactly describe the chaotic motion of the waterwheel, though they are more commonly expressed as

$$\dot{a_1} = \omega b_1 - K a_1 \quad (4)$$
$$\dot{b_1} = -\omega a_1 + q_1 - K b_1 \quad (5)$$
$$\dot{\omega} = -\left(\frac{\nu}{I}\right)\omega + \left(\frac{\pi g R}{I}\right) a_1 \quad (6)$$

where a_1 and b_1 are the cosine and sine Fourier coefficients of the fundamental mode of rotational coordinate of the wheel, respectively, and ω is the angular velocity of the wheel. We can lend physical insight to the a_1 and b_1 variables by recalling that $\cos(n\pi x/L)$ and $\sin(n\pi x/L)$ represent the orthogonal basis states for a Fourier decomposition. Thus a_1 gives a measure of the ratio of water on the left side of the wheel to that on the right, while b_1 gives a measure of the ratio of the water on the top of the wheel to that on the bottom [4].

In Equations 4–6, I is the moment of inertia of the wheel, ν is a rotational damping rate, g is the acceleration due to gravity, R is the radius of the wheel, K is the rate of leakage from the cups, q_1 is related to the inflow of water, and we have employed the transformation $x \to \omega/g$, $y \to (\pi g R/K\nu)a_1$, $z \to (b_1 - q_1/K)/b$ (*cf* [41]). Thus, we have written down a system of differential equations that describe the motion of the waterwheel, and we can use a time–stepping method to solve Equations 4–6 numerically, but we must use techniques from nonlinear stability analysis to make predictions about the asymptotic behavior of the system. What Lorenz found in 1963 is that there exist values for the parameters in his original system of equations that precluded stable fixed points and limit cycles, but for which the system's trajectory remained in a bounded set [26]. Such behavior is a hallmark of chaos.

A more illustrative example of chaos is the strange attractor. In short, the strange attractor is that bounded set in phase space on which a system's trajectory remains. More precisely, a strange attractor is an attractor which exhibits sensitive dependence on initial conditions, where an *attractor* is a minimal invariant set that attracts an open set of initial conditions. We can decode this definition by separating it into three terms: To attract an open set of initial conditions means that when a trajectory starts out in some open set that contains the attractor, that trajectory gets arbitrarily close to the attractor as $t \to \infty$. The word invariant means that once a trajectory is on the attractor, it does not leave, and the word minimal means that there is no proper subset of the attractor's set that is both invariant and attracts an open set of initial conditions [41].

In addition to the definition of a strange attractor given above, strange attractors can be distinguished from the attractors that describe linear processes by their fractal, or non–integer, dimension. In short, fractal dimension is an extension of the more familiar integer dimension to geometric figures for which the density of points around a given point changes over the figure. What we define as the fractal dimension of a strange attractor (which, incidentally, is approximately 2.06 for the Lorenz system) is a sort of average of the "local dimension" over the entire attractor [1].

The strange attractor for the Lorenz Equations is shown four ways in Figure 3: In the upper left panel, we show the attractor in three dimensions, and in each of the other three panels, we show the attractor projected onto one of the three possible planes. The motivation for showing the Lorenz attractor in this way is to illustrate its complexity as a geometrical object, as well as to demonstrate the risk in projecting an attractor onto too–low a dimension: Any of the two–dimensional images could appear to be a legitimate description of the dynamics, but the three–dimensional images shows that we need more than two dimensions to truly capture the dynamical trajectories. We are fortunate to have the differential equations for the Lorenz system, since knowledge of the underlying equations allows us to compute quantities such as the fractal dimension analytically. In most experimental applications, the only data are from a noisy time series sampled with finite precision for a finite length of time. In those cases, we must resort to numerics if we wish to characterize the attractor and move forward with analysis.

Fractal dimension is considered one of two invariants of the motion; the second is a class of numbers called global Lyapunov exponents. In much the same way as we can characterize a linear system by its Fourier spectrum, we can characterize a chaotic system by its fractal dimension and its global Lyapunov exponents [1]. In chaotic systems, points on an attractor diverge or converge exponentially quickly [41]. We know that a strange attractor is an attractor that exhibits sensitive dependence upon initial conditions. Thus, given an N–dimensional sphere of initial conditions, we can demand that the radius of the sphere be infinitesimally small and we will still have initial conditions that differ from each other enough that the sphere spreads out into an N–dimensional ellipsoid as time evolves. We can describe the time–dependent k^{th}–principle axis of the ellipsoid by $\delta_k(t) \sim \delta_k(0)e^{\lambda_k t}$ (we may consider $\delta_k(0)$ the distance of the k^{th} initial condition from the center of the initial

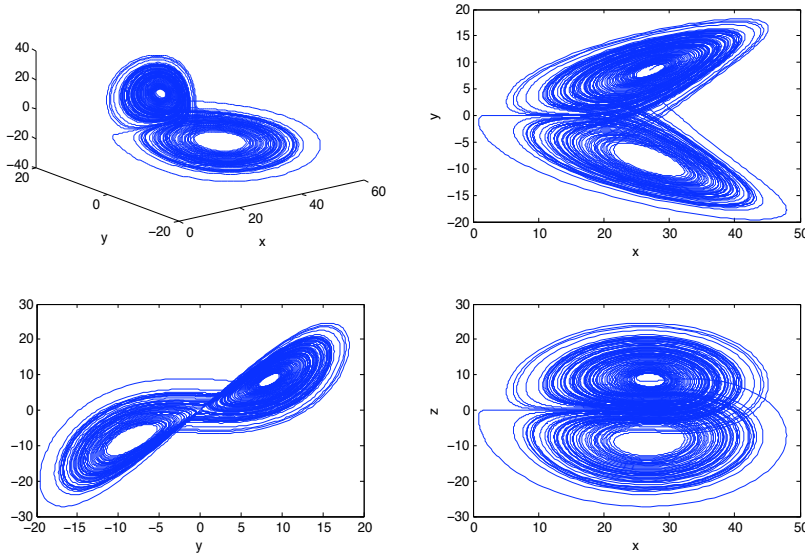

Figure 3: The strange attractor formed by the Lorenz Equations (equations 1–3), with $\sigma = 10$, $b = 8/3$, and $r = 28$. The upper left–hand panel shows a 3–D box plot of the set, while the other three panels show each of the three possible planes.

sphere) so that if at least one λ_k is positive, that principle axis will stretch the sphere in the k^{th} direction. Note that this exponential time dependence appears here as an ansatz, but is in fact predicted by Oseledec's multiplicative ergodic theorem [24]. If time evolves for long enough, the ellipsoid of initial conditions will be so stretched out over the attractor that we will have reached a point at which prediction breaks down [41]. We shall revisit the concept of Lyapunov exponents in §4

Now we can be exact when we speak of sunspot counts and solar activity as chaotic. When we hypothesize that solar activity follows a chaotic cycle, we imply that the magnitude of the current cycle depends in some way on the previous cycle or previous cycles, that the evolution through time of the solar cycle is sensitive to conditions at an earlier time, and that we can find an attractor that contains the information we need to understand the relevant dynamics. We are interested in describing the chaotic evolution of sunspot counts and other dynamical variables related to the Sun in order to determine which (possibly constant or periodic) physical drivers may be responsible for chaotic variations in solar activity, and then to use that knowledge to predict solar activity as far in the future as possible.

4 Nonlinear Analysis of Time Series Data

When presented with a time series that does not exhibit periodic behavior, we can still attempt to analyze the underlying dynamics by assuming that the data posses a nonlinear dependence. There exists a systematic method for uncovering dynamical dependence on multiple time scales known as attractor reconstruction, though determination of the correct value of certain parameters is not always simple. In order to suss out nonlinear time dependence from a vector $x(t)$ of scalar values sampled at discrete time points (i.e. a time series), we construct the N–dimensional vector

$$\mathbf{y}(t) = (x(t), x(t+\tau), ..., x(t+(N-1)\tau))$$

Therefore, we must know *a priori* the appropriate values of N and τ with which to construct $\mathbf{y}(t)$ (*cf* [41] and [1], but note that notations among this work and those two works differ). If the "embedding dimension" N is chosen to be too small, we can not construct $\mathbf{y}(t)$ such that it completely unfolds the dynamics of $x(t)$; if we choose N to be too large, noise will appear to be linked to the dynamics [11]. On the other hand, if we choose the "time delay" τ to be too small, the resultant components of $\mathbf{y}(t)$ will not be distinct enough to give us information about how the system evolves; if we choose τ to be too large, the intrinsic instability of the dynamics will cause $x(t)$ and $x(t+\tau)$ to act like random data points with respect to each other [1]. This intrinsic instability is, of course, a result of a positive maximum global Lyapunov exponent.

In our discussion of Lyapunov exponents above (see §3), we claimed that if at least one Lyapunov exponent is positive, and if time evolves "long enough", arbitrarily–close initial conditions will diverge so much that predictions based on the original information will break down. This amounts to two limiting processes: one as time goes to infinity, and the other as distance between nearby initial conditions goes to zero. Mathematically, we have

$$\lambda_j = \lim_{t\to\infty} \lim_{\delta_0 \to 0} \left(\frac{1}{t} \left| \frac{\delta(x_j, t)}{\delta_0} \right| \right) \tag{7}$$

Equation 7 is a *definition*, but it is not a very useful prescription for calculating the spectrum of global Lyapunov exponents from time series data. In effect, what we are doing when we calculate Lyapunov exponents is examining the stability of the dynamics to perturbations. Given a map $\mathbf{f}(\mathbf{y})$ that takes a point on the attractor $\mathbf{y}_i$ to the point $\mathbf{y}_{i+1}$, we consider a perturbation to first order:

$$\begin{aligned} \mathbf{y}_{i+1} + \delta_{i+1} &= \mathbf{f}(\mathbf{y}_i + \delta_i) \approx \mathbf{f}(\mathbf{y}_i) + \sum_{a,b} \frac{\partial f_a(\mathbf{y}_i)}{\partial x_b} \cdot \delta_i \\ \delta_{i+1} &\approx \sum_{a,b} \frac{\partial f_a(\mathbf{y}_i)}{\partial x_b} \cdot \delta_i \end{aligned} \tag{8}$$

where the last simplification comes from the definition of the map $\mathbf{f}(\mathbf{y}_i) = \mathbf{y}_{i+1}$ [1]. Thus, to first order, we are actually interested in the Jacobian matrix of $\mathbf{f}(\mathbf{y}_i)$. After applying this map a large number (call it n) of times, we can expect to learn about the stability of nearby initial conditions at long times. This last process relies on composing the Jacobian matrix with itself n times and forming the following matrix prescribed by the Oseledec multiplicative ergodic theorem mentioned in §3

$$\mathbf{O} = \left\{ \left[\sum_{a,b} \frac{\partial f_a(\mathbf{y}_i)}{\partial x_b} \right]^T \cdot \sum_{a,b} \frac{\partial f_a(\mathbf{y}_i)}{\partial x_b} \right\}^{1/2n} \tag{9}$$

Finally, the logarithms of the eigenvalues of $\mathbf{O}$ as $n \to \infty$ are the global Lyapunov exponents [2], [1].

What if n is not large? can we will learn information about the dynamics from the ratio inside the parentheses in Equations 7 or from the logarithms of the eigenvalues of $\mathbf{O}$? The answer is yes. These quantities, for finite time or n not large, are called the local Lyapunov exponents. Abarbanel *et al.* found that local Lyapunov exponents are relevant for predicting short–term dynamics or for characterizing the average variation of Lyapunov exponents over the attractor, as opposed to describing the long–term evolution of trajectories on the attractor [2]. The local Lyapunov exponents also provide a measure of the "heterogeneity" of the system in that they can characterize short–term chaotic behavior in an otherwise non–chaotic system [3].

5 The Solar Dynamo

Early analysis of the inner dynamics of the Sun focussed on hydrodynamic effects. Csada considered the fluid motion of the Sun, including differential rotation and meridional circulation, but neglected electromagnetic effects [12]. However, research has since shown that the electromagnetic induction that arises via differential rotation is the most effective mechanism for generating the toroidal fields seen in the solar dynamo [35]. In what follows, we will refer loosely to four main spherically–symmetric regions (R_S denotes the radius of the Sun): 1. the radiative zone, extending from the core out to $\sim 0.7R_S$, in which rotation is thought to be latitudinally uniform, 2. the convective zone, which lies between the radiative zone and the photosphere at $\sim 1R_S$ and exhibits latitudinally–varying rotational rates (differential rotation), 3. the tachocline, which lies at the interface between the radiative and convective zones, and 4. the overshoot layer, in which the convective zone spills briefly over into the radiative zone. Figure 4 shows a cartoon schematic of the inside of the Sun.

The early theory of Parker is regarded as seminal work in the development of solar dynamo theory [33], [32]. He acknowledged that the single relationship between a magnetic

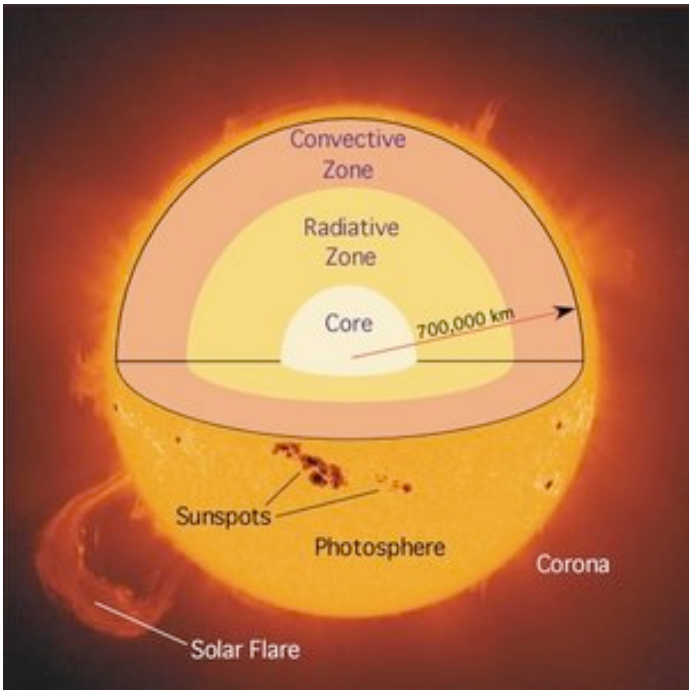

Figure 4: Cartoon representation of some major features of the Sun. The radiative zone extends out to $\sim 0.7R_S$, with the convective zone covering the balance out to the photosphere. The tachocline (not labeled) sits at the interface between the radiative and convective zones and the overshoot layer lies just below the tachocline. Image credit: Encyclopedia of the Earth (`http://www.eoearth.org/article/Solar_radiation`)

field and a fluid flow given by

$$\frac{\partial \mathbf{B}}{\partial t} = \nabla \times (\mathbf{v} \times \mathbf{B}) + \frac{1}{\mu\sigma}\nabla^2 \mathbf{B} \tag{10}$$

can not maintain both a poloidal magnetic field and a toroidal magnetic field, but found that an existing poloidal field *can* generate a toroidal field that would then regenerate the poloidal field through Equation 10 [32]. Given a poloidal magnetic field generated by a rotating conducting core, differential shearing can deform field lines by stretching them in the azimuthal direction, thereby generating a toroidal magnetic field (*cf* [35] and [30]). Once this toroidal field has been established, radially–rising cyclones in the radiative zone push radial field lines outward until they exhibit a non–axisymmetric bulge (imagine the capital letter omega: Ω). The cyclonic motion of these convective structures twists the bulged field line to give it a component parallel to the meridional plane, thereby regenerating the poloidal magnetic field [32]. We have come to refer to the generation

of toroidal magnetic fields via differential rotation as "the Ω effect" (this is in reference to the differential rotation, and is not to be confused with the Ω used to visualize radial stretching of toroidal field lines), and to the generation of poloidal magnetic fields via twisting of toroidal field lines as "the α effect" [20].

We have seen that the cyclonic flows proposed by Parker are crucial for generating the toroidal magnetic field at the interface between the radiative and convective zones, but the convective zone proper has its own characteristic flow that supports the solar dynamo. Choudhuri *et al.* developed a model that coupled the solar surface to the low–latitude base of the solar convective zone via large–scale meridional circulation [10]. Observational evidence suggests poleward meridional flows at the surface, while mass conservation suggests closure through equatorward flows at the base of the convective zone [9]. They noted that when the meridional circulation occurred on a timescale shorter than that of magnetic diffusion through the convective zone, rising loops of buoyant toroidal flux (a topic to be addressed in greater detail below) would produce butterfly diagrams in qualitative agreement with observation, and postulated that this effect is due to overcoming constraints imposed by coupling the two layers simply through diffusion. A decade later, [22] provided evidence that the solar dynamo is a diffusive dynamo. The meridional flow also acts upon decaying bipolar sunspot pairs to cause a net magnetic flux to move poleward, which, in turn, reverses the older polar field and builds up the poloidal field for the next cycle [30].

One final piece of the solar magnetic puzzle is the diffuse field that exists in the regions *not* occupied by sunspots. We will not consider this diffuse field here. However, the last few years of model and observational evidence have shown that this diffuse magnetic field gives important information about the dynamo process [9]. Therefore, we would be remiss to not mention it at all.

Now that we have established a foundation for understanding the solar dynamo process, we move onto sunspot formation proper. To begin our consideration of sunspot formation, we return to Parker, who remarked even in 1955 that the fact that overall visible changes in the corona are in step with magnetic activity suggests that "sunspots and prominences are not just individual isolated magnetic phenomena but are secondary effects of a general solar magnetic cycle" [32]. In fact, he had already acknowledged, earlier the same year, that if a closed loop of magnetic flux (hereafter referred to as a "flux loop" or "flux tube") contained in the toroidal magnetic field is in pressure equilibrium, then the external fluid pressure should be in balance with both the internal fluid pressure and the internal magnetic pressure [33] (*cf* [30]):

$$p_{ext} = p_{int} + \frac{B^2}{8\pi} \tag{11}$$

Thus, there will be a net (hydrostatic) buoyant force on the flux loop since $p_{int} < p_{ext}$ and the loop, or a portion thereof, will begin to rise. Furthermore, if the length of flux loop that begins to rise is twice the scale height of the medium, fluid will flow along the tube in an attempt to balance the hydrostatic pressure, thereby increasing the buoyancy and causing the loop to continue its rise [33]. Finally, if a buoyant flux tube rises high enough through

the convective zone to reach the photosphere, it will break through, as illustrated in Figure 5, and the visible result is a bipolar pair of regions of increased magnetic flux. The strong magnetic fields contained in the bipolar pair inhibit convective energy transport, thereby cooling the regions and causing them to appear darker than the surrounding photosphere [18]. Of course, these darker regions are what we know as sunspots.

The natural question to ask now is, "What causes toroidal flux tubes to form in the first place?" Without direct evidence of the inner workings of the Sun, we must rely upon models whose accuracy we gauge by assessing how well they produce observable features (e.g. emergence latitudes of sunspots and surface magnetic fields). A realistic starting point is unstable mechanical equilibrium in the thin convective overshoot region that lies just below the surface of the radiative zone. We suppose that the (toroidal) flux tube evolves through a series of stable mechanical equilibria, all the while being stretched azimuthally by differential rotation. At some point, the magnetic pressure inside the tube becomes so great that it begins to experience the magnetic buoyancy instability given by Equation 11 and it begins to rise [38]. The flux tube is also subject to instabilities arising from fluid undulations in the overshoot layer, so that the creation of unstable rising flux loops from toroidal field loops in mechanical equilibrium is not uncommon [5].

What did come as a surprise to researchers developing models of flux–tube generation and transport was the fact that, in order that these destabilized loops not be too strongly influenced by the Coriolis force (which would cause their emergence latitudes to be higher than those observed), the magnetic field in the overshoot layer had to be an order of magnitude greater than the equipartition value for kinetic and magnetic energy. This super–equipartition magnetic field also means that flux tubes in the overshoot layer will be even more unstable to undular perturbations [5].

Of course, the toroidal flux tubes could begin from *thermal* equilibrium as opposed to mechanical equilibrium, as many authors had been merely assuming through the late 1990s. However, Caligari *et al.* found that calculations starting from thermal equilibrium were unable to explain why flux loops with magnetic field strengths smaller than those observed should not also erupt through the photosphere. Their explanation, which they support with model results, relies on the fact that flux tubes beginning in mechanical equilibrium in the convective overshoot layer must develop the super–equipartition magnetic field before they become unstable and rise out of the overshoot layer [6]. This strong field further keeps the flux loops anchored in the overshoot layer (*ibid*).

The preceding is intended to provide a summary of developments in solar dynamo theory in order to build a context in which to place our analysis of sunspot counts and solar dynamics. Of course, we have fallen far short of providing an exhaustive review of the subject. There are many books, conference proceedings, and journal articles that treat observational or model data and the field is still quite active. In addition to the references listed here, the interested reader is referred to [14] for a good review of solar dynamo theory and models of sunspot formation within the rising–flux–tube paradigm.

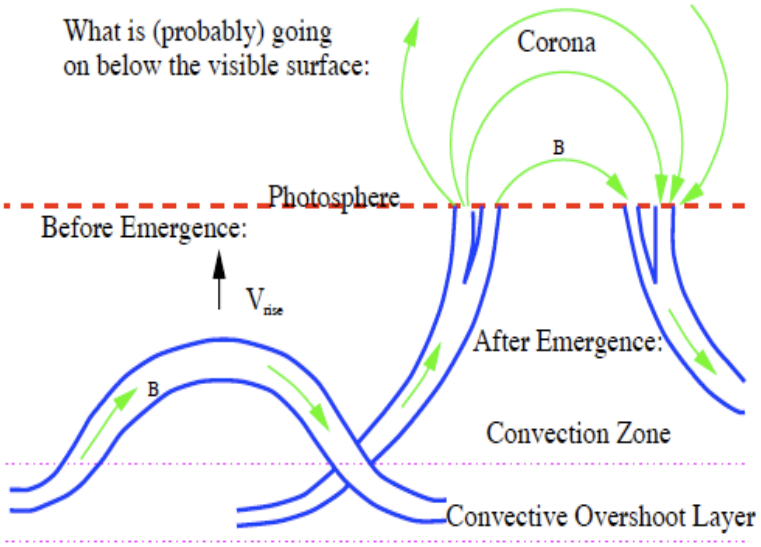

Figure 5: Cartoon representation of "what is (probably) going on below the visible surface" when a toroidal magnetic flux tube rises through the convective zone, then breaks through the photosphere to form a bipolar sunspot pair. Image credit: [14]

6 Data and Software

Let us now move on to analysis of sunspot counts and solar motion. Time series of sunspot counts are available on various time scales, with uncertainty in count increasing for dates further back in history. In this study, we use data of monthly sunspot counts spanning the time period 1749–2010 (i.e. roughly 6 years before the beginning of Cycle 1 through the present), available at `http://solarscience.msfc.nasa.gov/SunspotCycle.shtml`. The time series produced from these data is shown in Figure 6

Since we are also interested in the dynamics of the Sun, we obtained solar position and velocity data from the National Aeronautics and Space Administration Jet Propulsion Lab (NASA JPL) planetary ephemerides program, available at `http://ssd.jpl.nasa.gov/?ephemerides#planets`. An ephemeris is a data file giving the calculated positions of a celestial object at regular intervals throughout a period; the NASA JPL solar system ephemerides use Chebychev polynomials to interpolate between observations of objects in the solar system including the Sun and all nine planets. Observations are made at approximately 32–day intervals. Position and velocity data are available in reference to the center of the Sun or the center of gravity (also known as the barycenter) of the solar system. As with sunspot counts, data is available on different time scales, with varying precision. We use high–precision data spanning the period 1600–2099, where the data

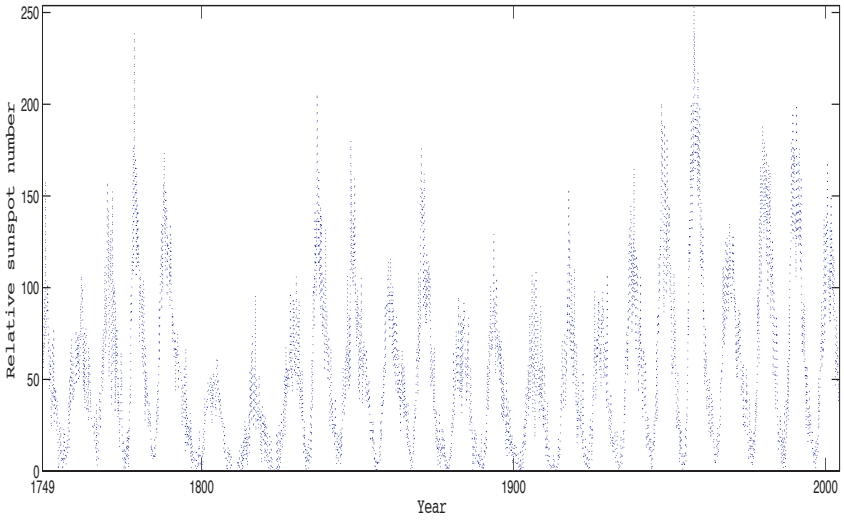

Figure 6: Monthly counts of sunspots since 1749.

beyond January 2011 are projected values.

We used numerical differencing of the velocity data to calculate the acceleration of the Sun about the barycenter of the solar system, which allowed us to calculate the force on the Sun through Newton's second law. The data for the magnitude of the Sun's acceleration ($|\mathbf{a}| = \sqrt{a_x^2 + a_y^2 + a_z^2}$) is plotted in Figure 7

In order to analyze the data, we employed algorithms written in the MATLAB© programing language, available at the MATLAB© file exchange (`http://www.mathworks.com/matlabcentral/fileexchange/`). The first algorithm, *chaosfn.m*, employs a neural network optimization approach to determine the spectrum of Lyapunov exponents for a given data series. The second function, *chaostest.m*, performs a statistical significance test on the maximum Lyapunov exponent returned by *chaosfn.m* to determine the probability that the returned value could have occurred by chance. This statistical test accounts for noise in the input data series. A third function, *embdsymplec.m* employs a symplectic geometry method to estimate the attractor embedding dimension that avoids short–comings of other embedding dimension algorithms [25]. In short, symplectic geometry is a natural (i.e. measure–preserving) way in which to perform the transformations necessary to determine the amount of mutual information contained in the data $x(t)$. Finally, a fourth function, *optim_m_tau.m* was used to confirm our own trial–and–error estimate of time delay τ. This function employs a differential entropy scheme, which is to say that it calculates the smallest value that contains the contains the dynamical variations. Thus it also

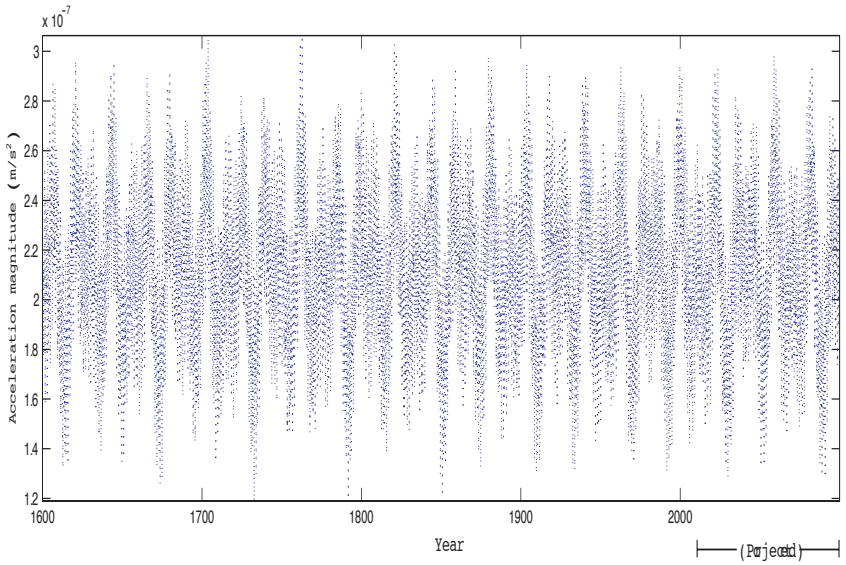

Figure 7: Magnitude of the Sun's acceleration spanning the period 1600–2099, where projected values are shown for dates after January 2011. The data were derived numerically from NASA JPL ephemerides.

returns the minimum attractor dimension.

7 Results

Estimation of the global Lyapunov exponents for sunspot number (s) and magnitude of solar acceleration (a) suggest that both time series are chaotic and have maximum global Lyapunov exponent $\lambda_s \approxeq 0.056$ month^{-1} and $\lambda_a \approxeq 0.079$ day^{-1}, respectively. The low values of these numbers with respect to unity suggest that divergence of nearby initial conditions is slow in time. However, there will still be a time after which prediction breaks down. The first result actually corroborates qualitatively a result found be Mundt *et al.* in 1991 [28]. Those authors used smoothed counts of sunspot numbers to derive an estimated average maximum global Lyapunov exponent $\lambda_s \approxeq 0.02$ month^{-1}. To our knowledge, this is the first time that an estimate for the maximum global Lyapunov exponent of the magnitude of solar acceleration (or any solar dynamic quantity, for that matter) has been reported. The finding is encouraging because it indicates the realm of analysis in which we ought to work when attempting to identify the mechanism underlying variation in sunspots and solar activity in general. That is to say that, provided this result stands up to further analysis, we need not spend our time trying to construct linear models in an attempt to

predict solar activity at arbitrarily–long times in the future.

Preliminary exploratory work by UNH Department of Mathematics and Statistics graduate student Yibin Pan suggested that $\tau = 16$ was a suitable value for the sunspot attractor delay time [31]. We considered this value reasonable, since Mundt *et al.* reported using a value of $\tau = 10$ for their smoothed data. The routine *optim_m_tau.m* returned the value $\tau = 17$. The routine also found that the minimum attractor dimension should be $m = 2$. For comparison, Mundt *et al.* estimated the embedding dimension of the sunspot attractor to be $N = 3$, then estimated the fractal attractor dimension to be $d \approxeq 2.3$ [28], which indicates that $m = 2$ for their study as well.

We initially attempted to naïevly reconstruct the solar dynamic attractors by assuming an embedding dimension of $N = 3$. In doing so, we found that $\tau = 366$ days seemed to best unfold the attractor. Happily, the routine *optim_m_tau.m* estimated the optimal delay to be $\tau = 361$, validating our trial–and–error value.

As for the attractor embedding dimension, the function *embdsymplec.m*, returned the values $N = 1$ and $N = 7$ for sunspot count and magnitude of solar acceleration, respectively. The first value seems to be outright wrong: the embedding dimension should be greater than the attractor dimension and should certainly not be smaller than the minimum attractor dimension! It is possible that the time series is too short for the algorithm to correctly identify N. With respect to the acceleration magnitude, however, we can share the following evidence that it may be correct, and not simply an artifact of numerical differentiation: We checked the value of N returned by *embdsymplec.m* for both the position and velocity time series provided by the NASA JPL ephemerides and found that $N = 3$ in each case. In order to derive acceleration data from velocity data, we used the Interactive Data Language (IDL) routine *deriv.pro*, which employs three–point Lagrangian interpolation. Therefore, we suspected that numerical differentiation may have introduced nonlinear correlations that were not representative of the underlying physics. To test this hypothesis, we performed the same numerical differentiation on the position ephemerides to obtain a second velocity time series. Using this as input to *embdsymplec.m* again resulted in the value $N = 3$, lending credence to the value of $N = 7$ obtained for acceleration magnitude.

8 Discussion

Certain previous studies have attempted to extract a direct planetary influence on solar activity by drawing links between planetary motions and sunspot counts. An early advocate for planetary tidal forcing was P. Jose, who took a cue from Isaac Newton to consider the Sun's complicated motion about the solar system barycenter [23]. He established that certain solar parameters of motion, most notably the Sun's instantaneous angular momentum about the solar system barycenter have a period of 178.7 years. He then examined data of sunspot counts and found a 178.55–year period cycle, which he concluded was a "more realistic period for the sunspot cycle" (*ibid*).

More recently, work by two separate authors has attempted to find similarities between periods in the sunspot cycle and periods derived from planetary orbits by summing, identifying harmonics, and calculating beats frequencies. In 2007, Charvátová identified a period in the motion of the inner planets that is similar to short–scale fluctuations in certain solar parameters identified by other researchers (see references therein), but did not propose a mechanism [8]. Scafetta noted numerous previously identified periods in the sunspot cycle ranging from a 60– to 65–year period to an 800– to 1200–year period [36] (and references therein). In that work, he claimed that planetary forcing at the period of some set of orbital harmonics could act to constrain solar dynamics to an "ideal cycle" about which solar activity fluctuates chaotically (*ibid*).

We have found, using a method described by Strogatz [41], an additional frequency attributable to planetary motion. That author identifies the compromise frequency of two coupled nonlinear oscillators as the "stable, phase–locked solution" approached by the trajectories of the combined system on the relevant attractor. Using stability analysis of the phase different between the two oscillators, he defines the compromise frequency as

$$\omega^* \equiv \frac{k_1\omega_2 + k_2\omega_1}{k_1 + k_2} \tag{12}$$

In order to explore the implications of this quantity to the problem of planetary forcing, we coupled Jupiter and Saturn (the two most massive planets in the solar system) through their mutual gravitational potential. Thus we identify the following quantities:

$$k_1 = \frac{Gm_J}{r_{JS}^2} \quad k_2 = \frac{Gm_S}{r_{SJ}^2}$$
$$\omega_1 = 2\pi f_J \quad \omega_2 = 2\pi f_S$$

where m_J and m_S are the respective masses of Jupiter and Saturn, $r_{JS}^2 = r_{SJ}^2$ is the square of the distance between Jupiter and Saturn, G is Newton's gravitational constant, and f_J and f_S are the respective orbital frequencies of Jupiter and Saturn. By substituting these quantities into Equation 12 and realizing that the period τ is related to the angular frequency ω by $\tau = 2\pi/\omega$, we were able to calculate the compromise period for Jupiter and Saturn:

$$\tau^* = \left(\frac{m_J + m_S}{\tau_J m_J + \tau_S m_S}\right) m_J m_S \approx 22\ yr \tag{13}$$

It is encouraging to find that this quantity is approximately equal to the magnetic cycle of the Sun.

In the previously referenced article by Scafetta, [36], the author cites a critique by Smythe and Eddy [39] of the planetary forcing argument. In response to [39], who argued that patterns of (quasi–periodic) tidal forces show no correlation with grand minima such as the Maunder Minimum, Scafetta notes that those authors did not account for the fact that solar variations must arise from coupling between the internal solar dynamo and external planetary forces [36].

A more recent critique of planetary forcing argues that the contributions to the acceleration on the Sun near the tachocline and convective overshoot region are negligible with respect to the acceleration on those regions due to the Sun's motion about the solar system barycenter alone [7]. The authors make a quite compelling argument, but they admit that they can not exclude the possibility that long–term planetary influences may contribute in a small but non–negligible way to internal motions of the Sun, albeit indirectly. As an example, they cite the curious Gnevyshev–Ohl rule, which states that when solar cycles are arranged in pairs in which the even–numbered cycle follows the odd–numbered cycle, there is a strong trend toward a higher number of sunspots in the odd cycle than in the even cycle (*cf* [29], [19]).

In fact, the acceleration on the center of mass of the Sun is quite small ($\mathcal{O}(10^{-7})$), as can be seen in Figure 7. However, we have seen that the solar dynamics relevant to the sunspot cycle occur at $\sim 0.7R_S$. Therefore, we are more concerned with the torque on fluid parcels in the convective overshoot layer, tachocline, and convective zone proper. A theoretical analysis by Wolff and Patrone suggests that coupling between the Sun's orbital motion and its angular acceleration about the solar system barycenter can increase the potential energy of certain correctly–positioned fluid elements [48]. The authors seem to imply that the planets must have some influence on this effect, since they, along with the Sun, define the barycenter of the solar system. It is worth noting that the authors of [7] were aware of this study but did not address it in detail.

The concept of short–term gravitational influences, as well as the notion that there may be portions of the solar cycle that are chaotic [22] but are constrained by deterministic oscillations (e.g. those of the planets as mentioned in [36], see paragraph 2 of this section) suggests that the next step toward understanding how solar dynamics relate to variations in solar activity is to characterize the local Lyapunov exponents of solar motion.

As a final note, future studies may benefit by examining activity in other stars, and using similarities and differences in theoretical structure of those stars, as well as the surrounding planetary environment, to support or eliminate mechanisms proposed for variation in solar activity. The "H–K" Project, conducted at the Mount Wilson Observatory in California, identified roughly a dozen slowly–rotating stars that exhibit quasi–periodic activity similar to that observed on the Sun [46]. Specifically, the comparison of rotation rate and activity cycle period of some K–class stars to those of our Sun (a G–class star) lead those authors to the conclusion that main sequence G– and K–class stars with certain parameters similar to the Sun's (e.g. age and rotation rate) can exhibit similar activity. However, observations of stellar activity have also revealed G–class stars with very little activity, so results are not yet conclusive (*ibid*).

9 Conclusions

To the typical observer, the Sun traces out a slow arc over the course of a day, and though the elevation of that arc may change drastically over the course of a year, or even disappear for some time at polar latitudes, it remains comfortingly predictable. Of course, those who work in space science (or know someone who does) may occasionally receive updates about potentially harmful or "geoeffective" solar activity (e.g. flares and CMEs), but even those reports do not do justice to the chaotic stew that boils below the photosphere. In this report, we have considered the history of the development of sunspot counts, the framework of chaos theory and nonlinear time series analysis, and current theoretical understanding of the solar dynamo. Furthermore, we have attempted to marry these topics toward the ultimate end of improving the space weather community's ability to reliably predict solar activity.

We have found that

1. The sunspot count is chaotic with a maximum global Lyapunov exponent $\lambda_s \approxeq 0.056$ month^{-1}, qualitatively confirming a previous result which used smoothed data [28],
2. The magnitude of solar acceleration is chaotic, with a maximum global Lyapunov exponent $\lambda_a \approxeq 0.079$ day^{-1}, and
3. The embedding dimension of solar acceleration magnitude is likely as high as $N = 7$, while results for the embedding dimension of sunspot counts were inconclusive.

The results presented here represent preliminary results in a study that requires a great deal of further work. Nevertheless, we hope to use these findings as a starting point to establish a mechanism by which chaotic solar dynamics produce observed sunspot counts, and to construct an algorithm that can reliably predict solar activity far enough into the future to be beneficial to life on Earth. We have acknowledged the attempts to attribute chaotic solar activity to planetary tidal forces [23], [8], and [36], as well as an attempt to characterize the chaos in sunspot counts [28]. However, we believe that no one has yet undertaken the task of connecting the mathematical framework of chaos with the physical framework of solar dynamo theory.

Acknowledgements

A portion of this research was supported by NH Space Grant. I am greatly indebted to my advisors Marc Lessard and Dawn Meredith for enlightening conversations, useful critiques, and endless patience. This work also benefited from helpful conversations about nonlinear dynamics with Dr. Kevin Short and Yibin Pan of the University of New Hampshire Department of Mathematics and Statistics, and about the solar dynamo with Dr. Terry Forbes of University of New Hampshire Institute for the Study of Earth, Oceans, and Space.

References

[1] Henry D. I. Abarbanel. *Analysis of Observed Chaotic Data.* Springer: New York, 1996.

[2] Henry D. I. Abarbanel, R. Brown, and M. B. Kennel. Variation of Lyapunov Exponents on a Strange Attractor. *J. Nonlin. Sci.*, 1, 1991.

[3] Barbara A. Bailey, Stephen Ellner, and Douglas W. Nychka. Chaos with Confidence: Asymptotics and Applications of Local Lyapunov Exponents, 1997.

[4] Gabriel Benel. Mechanical Analogs to the Lorenz Equations. Masters of Engineering Project Report, 2003.

[5] P. Caligari, F. Moreno–Insertis, and M. Schüssler. Emerging Flux Tubes in the Solar Convection Zone. I. Asymmetry, tilt, and emergence lattitude. *Astrophys. J.*, 441, 1995.

[6] P. Caligari, M. Schüssler, and F. Moreno–Insertis. Emerging Flux Tubes in the Solar Convection Zone. II. The influence of initial conditions. *Astrophys. J.*, 502, 1998.

[7] Dirk K. Callebaut, Cornelis de Jager, and Silvia Duhau. The influence of planetary attractions on the solar tacholine. *J. Atmos. Sol.–Terr. Phys.*, 80, 2012.

[8] I. Charvátová. The prominent 1.6-year periodicity in solar motion due to the inner planets. *Ann. Geophys.*, 25, 2007.

[9] A. R. Choudhuri. The solar dynamo as a model of the solar cycle. In *Dynamic Sun.* Cambridge Press, 2003.

[10] A. R. Choudhuri, M. Schüssler, and M. Dikpati. The solar dynamo with meridional circulation. *Astron. Astropys.*, 303, 1995.

[11] Bian Chun-Hua and Ning Xin-Bao. Determining the minimum embedding dimension of nonlinear time series based on the prediction method. *Chin. Phys. B*, 13, 2008.

[12] Imre Csada. The differential rotation and the large–scale meridional motion of the stars. *Contributions from the Konkoly Observatory*, 22, 1949.

[13] John A. Eddy. The Maunder Minimum. *Science*, 129(4245):1189–1202, 1976.

[14] G. H. Fisher, Y. Fan, D. W. Longcope, M. G. Linton, and A. A. Pevtsov. The Solar Dynamo and Emerging Flux - (Invited Review). *Solar Phys.*, 192, 2000.

[15] A. A. Hady. Descriptive study of solar activity sudden increase and Halloween storms of 2003. *Journal of Atmospheric and Solar-Terrestrial Physics*, 71, 2009.

[16] F. Halberg, G. Cornlissen, R. B. Sothern, J. Czaplicki, and O. Schwartzkopff. Thirty–Five–Year Climatic Cycle in Heliogeophysics, Psychophysiology, Military Politics, and Economics. *Izvest. Atmos. Ocean.*, 46, 2010.

[17] George E. Hale. On the Probable Existence of a Magnetic Field in Sunspots. *Astrophys. J.*, 1908.

[18] Arnold Hanslmeier. The Sun and Space Weather. In *Heliophysical Processes*. Springer: New York, 2010.

[19] David Hathaway. The Solar Cycle. *Living Rev. Solar Phys.*, 7, 2010.

[20] H. Hotta and T. Yokoyama. Importance of surface turbulent diffusivity in the solar flux–transport dynamo. *Astrophys. J.*, 709, 2010.

[21] William J. M. Hrushesky, Robert B. Sothern, Jovelyn Du-Quiton, Dinah Faith T. Quiton, Wop Rietveld, and Mathilde E. Boon. Sunspot Dynamics Are Reflected in Human Physiology and Pathophysiology. *Astrobio.*, 11, 2011.

[22] Jie Jiang, Piyali Chatterjee, and Arnab Rai Choudhuri. Solar activity forecast with a dynamo model. *Mon. Not. R. Astron. Soc.*, 381, 2007.

[23] Paul D. Jose. Sun's Motion and Sunspots. *Astronom. J.*, 70, 1965.

[24] Jim Kelliher. Oseledec's Multiplicative Ergodic Theorem. Notes for the Fall 2002 Junior Geometry seminar at UT Austin, revised and updated, 2011.

[25] M. Lei, Z. Wang, and Z. Feng. A method of embedding dimension estimation based on symplectic geometry. *Phys. Lett. A*, 303, 2002.

[26] Edward N. Lorenz. Deterministic Nonperiodic Flow. *Journal of the Atmospheric Sciences*, 20:130–141, 1963.

[27] E. Walter Maunder. Note on the Distribution of Sun–spots in Heliographic Latitude, 1874–1902. *Mon. Not. R. Astron. Soc.*, 64, 1904.

[28] Michael D. Mundt, II Maguire, W. Bruce, and Robert R. P. Chase. Chaos in the Sunspot Cycle: Analysis and Prediction. *J. Geophys. Res.*, 96(A2):1705–1716, 1991.

[29] Y. A. Nagovitsyn, E. Y. Nagovitsyna, and V. V. Makarova. The Gnevyshev–Ohl rule for physical parameters of the solar magnetic field: The 400–year interval. *Astronomy Letters*, 35, 2009.

[30] Dibyendu Nandy. Dynamo Processes. In *Heliophysical Processes*. Springer: New York, 2010.

[31] Yibin Pan. personal communication, 2012. Univ. of New Hamp. Dept. of Mathematics and Statistics.

[32] Eugene N. Parker. Hydromagnetic dynamo models. *Astrophys. J.*, 122, 1955.

[33] Eugene N. Parker. The formation of sunspots from the solar toroidal field. *Astrophys. J.*, 121, 1955.

[34] P. Preka-Papadema, X. Moussas, M. Noula, H. Katranitsa, A. Theodoropoulou, C. Katsavrias, C. Vasiliou, E. Kontogeorgou, S.-M. Tsaliki, K. Kailas, and T. Papadima. The Effect of Helio-Geomagnetic Activity on the Proceedings in the Emergency Department of Two Greek Hospitals. In A. Angelopoulos and T. Fildisis, editors, *American Institute of Physics Conference Series*, volume 1203 of *American Institute of Physics Conference Series*, pages 893–898, 2010.

[35] Günther Rüdiger. *Differential Rotation and Stellar Convection.* Gordon and Breach Science Publishers: New York, 1989.

[36] Nicola Scafetta. Multi–scale harmonic model for solar and climate cyclical variation throughout the Holocene based on Jupiter–Saturn tidal frequencies plus the 11–year solar dynamo. *J. Atmos. Sol.–Terr. Phys.*, in press, 2012.

[37] Carolus J. Schrijver and George L. Siscoe, editors. *Space Storms and Radiation: Causes and Effects.* Heliophysics. Cambridge University Press, 2012.

[38] M. Schüssler, P. Caligari, A. Ferriz–Mas, and F. Moreno–Insertis. Instability and eruption of magnetic flux tubes in the solar convection zone. *Astron. Astropys.*, 281, 1994.

[39] Charles M. Smythe and John A. Eddy. Planetary tides during the Maunder Sunspot Minimum. *Nature*, 266, 1977.

[40] Willie Wei-Hock Soon and Steven H. Yaskell. *The Maunder Minimum and the Variable Sun–Earth Connection.* World Scientific Press, 2003.

[41] Steven H. Strogatz. *Nonlinear Dynamics and Chaos.* Westview Press, 1994.

[42] McKenna–Lawlor Susan, P. Gonçalves A. Keating, G. Reitz, and D. Matthiä. Overview of energetic particle hazards during prospective manned missions to Mars. *Planet. Space Sci.*, 63, 2012.

[43] E. K. Sutton, J. M. Forbes, R. S. Nerem, and T. N. Woods. Neutral Density Response to the Solar Flares of October and November, 2003. *Geophys. Res. Lett.*, 33, 2006.

[44] Z. Švesta. Solar activity. In *Dynamic Sun.* Cambridge Press, 2003.

[45] They Might Be Giants. Here Comes the Science.

[46] John H. Thomas and Nigel O. Weiss. *Sunspots and Starspots*. Number 46 in Cambridge Astrophysics Series. Cambridge University Press, 2008.

[47] Steven T. Thornton and Jerry B. Marion. *Classical Dynamics of Particles and Systems*. Harcourt Brace Jovanovich, third edition, 1988.

[48] Charles L. Wolff and Paul N. Patrone. A new way that planets can affect the sun. *Solar Phys.*, 266, 2010.